KeAi
CHINESE ROOTS
GLOBAL IMPACT

Contents lists available at ScienceDirect

Journal of Holistic Integrative Pharmacy

journal homepage: www.keaipublishing.com/en/journals/journal-of-holistic-integrative-pharmacy



Potential small-molecule compounds and targets for Alzheimer's disease: Integrating bioinformatics analysis and *in vitro* verification



Jiaorong Zheng^{a,f}, Deti Peng^{b,f}, Zhigao Liao^{c,d,f}, Min Hong^{a,*}, Weiqu Yuan^{e,**}, Danping Huang^{a,***}

- ^a The First Affiliated Hospital of Guangdong Pharmaceutical University, Guangzhou, 510030, China
- b Department of Hepatology, Shenzhen Traditional Chinese Medicine Hospital, The Fourth Clinical Medical College of Guangzhou University of Chinese Medicine, Shenzhen, 510008, China
- ^c Department of Neurology, Xianning Hospital of Traditional Chinese Medicine, Xianning, 437100, China
- ^d The First Clinical College of Hubei University of Chinese Medicine, Wuhan, 430061, China
- ^e Department of Acupuncture, Shenzhen Traditional Chinese Medicine Hospital, The Fourth Clinical Medical College of Guangzhou University of Chinese Medicine, Shenzhen, 510008, China

ARTICLE INFO

Keywords: Alzheimer's disease Bioinformatics analysis Differential expression genes Molecular docking CREBBP Prochlorperazine Small-molecule compounds

ABSTRACT

Objective: Alzheimer's disease (AD) is a common neurodegenerative disorder characterized by progressive memory decline and cognitive dysfunction. The specific pathogenesis of AD remains unclear. This study aimed to explore the crucial genes and therapeutic small-molecule compounds in AD via integrated bioinformatics analysis, molecular docking, and *in vitro* verification.

Methods: The gene dataset GSE122063, including 12 samples from patients with AD and 11 non-demented control samples, was downloaded from the Gene Expression Omnibus (GEO) database. The online tool GEO2R was used to analyze differentially expressed genes (DEGs). Functional enrichment analysis of the DEGs was performed using DAVID and ClueGo databases. A protein-protein interaction network was constructed using the STRING database and visualized in Cytoscape. Potential small-molecule compounds for AD therapy were screened using the Connectivity map database. The crucial genes in a rat model of AD were confirmed by RT-PCR. Molecular docking of the screened crucial genes and small-molecule compounds was further performed to identify potential therapeutic drugs for AD.

Results: A total of 1145 DEGs were identified, which were enriched in intracellular protein transport, cell cycle, establishment of protein localization to membrane, and so on. Eight hub genes, including RPS29, CREBBP, ANAPC10, ANAPC4, MAGOHB, TCEB2, RPL10A, and SEC61A1, were identified in the protein-protein interaction network. The MAPK signaling pathway was closely related to AD. Furthermore, increased expression of CREBBP was confirmed in the rat model of AD, and molecular docking revealed that CREBBP exhibited the strongest binding affinity with prochlorperazine.

Conclusion: CREBBP was identified as a crucial hub gene and might serve as a potential target for AD. Prochlorperazine, which exhibited strong binding to CREBBP, showed potential as a therapeutic drug in AD.

Peer review under the responsibility of Editorial Board of Journal of Holistic Integrative Pharmacy.

^{*} Corresponding author. The First Affiliated hospital of Guangdong Pharmaceutical University. No.19 Nonglinxia Road, Yuexiu District, Guangzhou, 510030, Guangdong Province, China.

^{**} Corresponding author. Department of Acupuncture, Shenzhen Traditional Chinese Medicine Hospital, The Fourth Clinical Medical College of Guangzhou University of Chinese Medicine, No. 1 Fuhua Road, Futian District, Shenzhen, 510008, Guangdong Province, China.

^{***} Corresponding author. The First Affiliated hospital of Guangdong Pharmaceutical University. No.19 Nonglinxia Road, Yuexiu District, Guangzhou, 510030, Guangdong Province, China.

E-mail addresses: hmin130@163.com (M. Hong), szyuanweiqu@163.com (W. Yuan), huangdanping@gdpu.edu.cn (D. Huang).

^f Jiaorong Zheng, Deti Peng and Zhigao Liao contributed equally to this work.

1. Introduction

Alzheimer's disease (AD) is a common neurodegenerative disorder characterized by progressive decline of memory function, cognitive dysfunction, and declines in language and social function, and further develops personality changes and loss of viability until death. ^{1,2} As the population ages, AD has emerged as one of the most serious diseases endangering the health of the elderly and is now recognized as a major public health problem worldwide.³ There are several hypotheses that have been proposed to explain the pathogenesis of AD, such as involvement of the inflammatory response, amyloid β -protein (A β), Tau protein accumulation, and gene mutation theories.⁴ Pathway analyses have shown that pathways related to cholesterol metabolism, immune response, neuronal differentiation, and inflammation-related signaling pathways are strongly associated with AD pathogenesis. 5,6 Recently, a network analysis of 1647 postmortem brain tissues from individuals with late-onset AD and healthy controls revealed that genes regulated by TYROBP are upregulated in AD. TYROBP plays a role in innate immunity, specifically mediating microglia in the brain.⁸ However, the exact pathogenesis of AD remains incompletely understood. Current clinical treatments for AD, such as cholinesterase inhibitors and other drugs, can improve the AD symptoms⁹ but can't effectively halt disease progression and are often limited by uncertain efficacy and adverse side effects. Therefore, a better understanding of the molecular mechanisms underlying AD pathogenesis and the development of novel therapies are urgently needed.

Bioinformatics analysis has undergone significant advancement in the past decades, which is widely applied in molecular biology experiments and clinical practice. For example, Srikant Rangaraju et al. conducted weighted co-expressed network analysis (WGCNA) to explore highly co-expressed genes of neuroinflammatory and neurodegenerative disease mouse models, further establishing a potential transcriptomic framework of microglial activation in neurodegeneration and providing guidance for targeting neuroinflammation for AD. ¹⁰ Bo Yang et al. performed microarray analysis to identify expression patterns of dysregulated lncRNAs in the hippocampus of AD model and constructed a lncRNA-mRNA network to elucidate the potential role of lncRNAs in AD. ¹¹ These studies demonstrate that bioinformatics analysis is a powerful tool for exploring AD pathophysiology and treatment strategies.

Molecular docking is a valuable approach in structural molecular biology and computer-assisted drug design. Predicting the predominant binding mode(s) between a ligand and a protein of known three-dimensional structure is the ultimate goal for ligand-protein docking. This method provides structural insights into ligand-protein interactions, which is crucial in virtual high-throughput screening and drug discovery. For instance, Mubashir Hassan et al. identified the binding pattern of clinical drugs for AD including AZD3293 and Solanezumab, against their target proteins through molecular docking and found AZD3293 showed a better therapeutic efficacy for AD than Solanezumab. Similarly, An Zhou et al. carried out molecular docking analysis to study tacrine derivatives and their AChE-inhibitory activities and identified the key residues, including Tyr70, Trp84, Tyr121, Trp279, and Phe330, of the binding site of AChE, providing a basis for designing novel AChE inhibitors. Identified the control of the signing novel AChE inhibitors.

In this study, we identified DEGs between AD samples and non-demented controls using GEO2R online tool applied to the GSE122063. We then performed GO and KEGG enrichment analyses to explore their functional implications. Next, crucial genes were recognized following establishment of a protein-protein interaction (PPI) network and validated in an AD model through qPCR array. Finally, potential therapeutic small molecule compounds for AD were further identified according to screened crucial genes through molecular docking approach. Our results indicate that prochlorperazine, which shows the strongest binding affinity for the hub gene *CREBBP*, may be a promising candidate for AD treatment.

2. Materials and methods

2.1. Microarray profiling

The original data of gene expression profile GSE122063, based on the platform of GPL16699, was collected from Gene Expression Omnibus (GEO, https://www.ncbi.nlm.nih.gov/geo) in the National Center for Biological Information (NCBI). The array data was submitted in 2018 and updated in 2019 by Erin Catherine McKay et al. ¹⁵ GSE122063 included cortex tissue obtained from 8 patients with vascular dementia, 12 patients with AD and 11 normal patients. More detailed information was recorded in the previous study. ¹⁵

2.2. DEGs analysis

GEO2R is an online tool (http://www.ncbnlm.nih.gov/geo/geo2r/) 16 used for identifying and analyzing differentially expressed genes in a GEO series under the same experimental conditions. We analyzed DEGs between 12 AD cases (without infarcts) and 10 controls from GSE122063, excluding all VaD samples. The original study confirmed AD cases lacked vascular pathology and VaD cases showed minimal AD pathology. 15. $|\log 2FC| \geq 1$ and adjusted P value < 0.05 were set as thresholds for screening DEGs. Gene ID number was transformed into gene name by the Database of Annotation Visualization and Integrated Discovery (DAVID) online database. 17,18 Heat map was generated using SangerBox (V1.0.8) and the volcano plot was plotted by online tool omicShare (https://www.omicshare.com/tools/Home/Soft/search).

2.3. Functional enrichment analysis

ClueGo is a cytoscape plugins for visualizing large gene clusters in a functionally grouped network. 19 The ClueGO network was established with kappa statistical algorithm to clarify the relationships between the terms according to the similarity of associated genes of different terms. It can analyze both single clusters and multiple cluster functions based on the newest data from Gene Ontology, KEGG, WikiPathways and Reactome and other databases. GO term enrichment analysis in AD was performed with ClueGo as described previously 20 DAVID online database is an integrated biological knowledgebase and analytic tools for systematically extracting biological value from numerous gene lists to uncover specific functional genes. 17,18 KEGG pathway was analyzed using DAVID database. P < 0.05 was considered significant difference.

2.4. PPI network analysis

Protein-protein interactions (PPI) of DEGs were extracted from the Search Tool for the Retrieval of Interacting Genes (STRING 11.0; htt ps://string-db.org/). STRING is a database with weighted physical and functional protein interactions based on multiple data sources and provides information associated with predicted and experimental interrelationships of proteins. DEGs were inputted to STRING database and protein pairs with a combined score of > 0.7 were selected. PPI network was established in Cytoscape v3.7.1 (http://www.cytoscape.org/). Nodes with a higher degree were considered as crucial nodes. Sub-modules included in the PPI network were identified with Molecular Complex Detection (MCODE; V 1.5.1). Criteria for sub-modules were set as follows: number of nodes > 12 and MCODE score > 8. Further enrichment analysis for the sub-modules was performed by DAVID, ClueGo as described above.

2.5. Drug-like small molecules

The Connectivity map (CMap, https://portals.broadinstitute.or g/cmap/).²³ including genome-wide transcriptional expression information from cultured human cells treated with bioactive small molecules and simple pattern-matching algorithms, has been widely applied

in the field of functional connections finding between drugs, genes, and diseases through common gene-expression alterations. After topology analysis, screened DEGs of AD were imported into CMap. The small molecule compounds related to AD disease were identified by comparing the expression patterns of key genes and specific genes interfered by small molecules in CMap. Criterion for selected small molecules was a score > 0.9.

2.6. $A\beta_{1-42}$ -infused rat model

All animal experiment procedures using rats were approved by the Animal Experiment Administration Committee of Hubei University of Traditional Chinese Medicine (No.42000600030515). A total of 12 three-month-old SPF male SD rats, weighing 220 \pm 20 g, purchased from Hubei Lab Animal Research Center, were reared in an SPF-level animal center at Experimental Animal Center of Hubei University of Traditional Chinese Medicine under the conditions of no pathogens with an ambient temperature of 21 $^{\circ}\text{C}\text{--}24~^{\circ}\text{C}$ and relative humidity of 40%– 60% and given sterilized food and water. A 12-h day with night cycle was maintained in the rearing facility. All rats were given habituation for 7 days before the formal experiments with normal food and water. A preliminary screening was performed using the Y-maze test to exclude rats with congenital dementia. The rats were randomly divided into two groups (n = 6 per group): the model group and the control group. According to previous study, we established a validated AD model through intra-cerebroventricular (ICV) injection of $A\beta_{1-42}$ peptide (AOBOX, Beijing, China) into the cerebral ventricles of the animals. Briefly, we injected 10% chloral hydrate (4 mL/kg) into the animals intraperitoneally (i.p.) to induce anesthesia and fixed the animals on a stereotactic frame. 5 μ L A β_{1-42} peptides were injected into the bilateral cerebral ventricle by a stainless steel cannula. The coordinates of injection were 1.1 mm anterioposterior from bregma, 2.2 mm lateral to the sagittal suture, and 3.0 mm beneath the dura. 11,24-26 In contrast, the control group received the same surgical procedure and an equal volume (5 μ L) of sterile normal saline instead of $A\beta_{1.42}$ peptide.

2.7. Morris water maze (MWM) test

To evaluate the spatial learning and memory deficits of SD rats, we conducted MWM test as previously described.²⁷ In brief, water mazes consisted of a blank circular pool with 120 cm in diameter and 40 cm in depth and were filled with water (25 \pm 1 $^{\circ}$ C). The apparatus was divided into four equal quadrants by four poles along the circumference of the basin. A round platform with 12 cm in diameter) was fixed in one of the quadrants of the pool and immersed 1 cm below the water surface. Training on finding the platform was conducted 5 times per day (90 s/time) and lasted for 5 days. Escape latency was calculated based on the time spent in finding a fixed platform. Twenty hours after spatial test, the platform was removed and the animals had to search for the platform in the apparatus; The swimming times across the platform area were recorded. The movements of the animals were recorded with an overhead video recorder connected to the tracking system (Stoelting Co., USA). After the Morris water maze test, all animals were sacrificed via decapitation under anesthesia. The hippocampal tissues were flash frozen and stored in liquid nitrogen before analysis.

2.8. Western blot

To investigate the representative protein expression of AD, the brain tissue was first lysed in RIPA buffer (Sigma, St. Louis, MO) containing a protease inhibitor mixture (Roche Diagnostics, IN). Protein concentration was detected with the bicinchoninic acid assay (Thermo Fisher Scientific, Bonn, Germany). A total of $50~\mu g$ protein lysates were used for sodium dodecyl sulfate polyacrylamide gel electrophoresis, then transferred to a polyvinylidene fluoride microporous membrane (Millipore, Billerica, MA, USA). Following saturation with 5% nonfat milk, the

membranes were incubated with primary antibodies overnight at 4 °C and secondary antibodies for 2 h at room temperature. Then, target antibodies were detected by the enhanced chemiluminescence detection reagents (Tanon, Shanghai, China). Signals were captured by the Image Lab software. Primary antibodies selected in this study were as follows: $A\beta$, p-Tau, Tau, and Actin. All primary antibodies were purchased from Proteintech company (Chicago, USA).

2.9. Histopathological analysis

Fresh tissues were collected for paraffin blocks. Serial 10 μ m hippocampal sections underwent H&E staining and immunohistochemistry (IHC). H&E staining and IHC were performed using standard techniques. In brief, the sections were rehydrated with a series of ethanol with different concentrations. For H&E staining, 10% hematoxylin was used for nucleus staining and 1% eosin was used for cytoplasm visualization at room temperature. For IHC, phosphorylated tau was probed with phosphorylated tau (1:200) mouse monoclonal antibody, and $A\beta_{1.42}$ was probed (1:200) with rabbit polyclonal specific anti- $A\beta_{1.42}$ antibody overnight at 4 °C. The labelled cells were visualized with DAB staining. Dehydration process was carried out by ascending alcohol solution prior to hyalinization with xylene. At last, the sections were sealed and evaluated with light microscopy.

2.10. Real-time PCR analysis

RT-PCR array was performed to analyze transcript expression of candidate genes. Briefly, total RNA was extracted using TRIzol reagent (Invitrogen, Carlsbad, CA, U.S.). Reverse transcriptions were carried out with 1 μ g of total RNA using PrimeScript® RT Master Mix Perfect Real Time (Takara, Japan) according to the instructions. Transcript expression quantifications were determined using SYBR® Premix Ex TaqTM II (Perfect Real Time, Takara, Japan). Signals of target genes were captured by ABI Quant Studio 7 Flex Real-Time PCR System. All mRNA quantifications were normalized against β -actin. Primers used for PCR amplifications were synthesized by Sangon Biotech Co., Ltd (Shanghai, China) and shown in Table 1.

2.11. Molecular docking

The AutoDock v4.2.6 and AutoDockTools v1.5.6 (ADT) software²⁸ were applied to calculate and analyze the optimal binding conformation and binding energy (BE) between the top 12 small molecule compounds from CMap and *CREBBP*. The three-dimensional structures of the 12 selected small molecules were downloaded from NCBI PubChem and the crystal structure of CREBBP (PDB ID: 6YIL) was obtained from the

Table 1Primers used for real-time PCR in this study.

Name	Direction	Primer (5' -3')		
RPS29	Forward	TGGGTCACCAGCAGCTCTACTG		
	Reverse	CGGAAGCACTGTCGGCACATG		
CREBBP	Forward	GACGAGAGCAAGCGAATGGAGAG		
	Reverse	TGGGCAACTTGGCAGGCTTTC		
ANAPC10	Forward	TGGAGAGGACAGCAACAGTGAGG		
	Reverse	GAGAGCCATCGGATTGCCAGTAAG		
ANAPC4	Forward	ATGGGACGTGAGGGAAGAGACAG		
	Reverse	CATCAAGCCTGGTGGAGCAAGTC		
MAGOHB	Forward	GCCGGACGGGAAGCTTAGATATG		
	Reverse	CACAGAGCGTCGTCCTCTTTG		
TCEB2	Forward	CAAGGAGTCGAGCACGGTGTTC		
	Reverse	GTGAAGCCACATTCGCCCAGAG		
SEC61A	Forward	GAAGGAGCAGCAGATGGTGATGAG		
	Reverse	AGGAAATCAGCCAGGACAGAGAGG		
RPL10A	Forward	GCAAGTTTCTGGAGACGGTGGAG		
	Reverse	GGTGCCCGAGAAGCGTTTGTC		
β -actin	Forward	CCCGCGGAGTACAACCTTCT		
	Reverse	CGTCATCCATGGCGAACT		

Protein Data Bank for molecular docking studies (http://www.rcsb.org/pdb/).²⁹

Semi-flexible molecular docking was utilized to optimize the calculating parameters, including the location and size of binding sites, flexible residues, and the optimal binding conformations of the 12 small molecule compounds in CREBBP. First, the receptor structures of CREBBP were prepared by adding polar hydrogen atoms, calculating the addition base charge, and specifying the AD4 atom type in ADT. Second, the grid box was chosen to cover the residues in binding site, using the following parameters to calculate through the AutoGrid program: set the box size and center the ligand; the grid spacing is set to 0.375 Å. Third, docking between the 12 small molecule compounds and CREBBP in binding site was performed, respectively. The parameters of Lamarck's genetic algorithm (LGA), used to optimize the conformation of the 12 small molecule compounds and CREBBP in each binding pocket, were listed as follows: the number of individuals in population, the maximum number of energy evaluations, the maximum number of generations, and the number of GA runs were set as 50, 5.0×10^6 , 2.7×10^4 , and 50, respectively, and other parameters were default. ADT, DS, and PyMol software were employed to visualize the docking results. Flexible dockings were then applied to further calculate the lowest binding energy (LBE) of each complex. The residues which had interactions with the 12 small molecule compounds after semi-flexible docking were defined as flexible residues (Supplement 2- Fig. 1). The location and size of grid box, and the docking parameters were the same as described above.

2.12. Statistical analysis

The data were presented as mean \pm standard deviation (SD). Multiple groups were compared using a one-way analysis of variance (ANOVA), followed by Dunnett's *t*-test. The threshold for statistical significance was set at a *P*-value less than 0.05 (P < 0.05).

3. Results

3.1. DEG analysis

Microarray data was used to analyze the different expression levels of genes in AD samples relative to those in normal group. Result of GEO2R analysis showed that a total of 1445 DEGs, including 909 upregulated and 536 downregulated genes, were identified based on the cut-off criteria (adjusted P value < 0.05 and $|log2FC| \ge 1$) (Supplement 1). Then, DEGs were inputted into SangerBox and online tool omicShare

to create a heat map and a volcano plot, respectively. The volcano plot was shown in Fig. 1A and the heat map of the top 100 up- and down-regulated DEGs was shown in Fig. 1B.

3.2. GO enrichment analysis

To predict the biological functions of the DEGs, we conducted the functional enrichment analysis of GO terms, including biological process (BP), cell component (CC), and molecular function (MF), using ClueGo. As shown in Fig. 2A and B, the DEGs were mapped to 81 different biological processes. The prominent terms were intracellular protein transport (38.24%), cell cycle (20.59%) and establishment of protein localization to membrane (11.76%). Cell component participated in 39 different terms (Fig. 2C), and the most enriched terms were clathrin vesicle coat (46.15%), nuclear part (15.38%) and catalytic complex (12.82%) (Fig. 2D). Additionally, GO molecular function was associated with 11 terms (Fig. 2E) and the major items were ubiquitin-protein transferase activity (36.36%), clathrin heavy chain binding (18.18%) and transcription coregulatory activity (18.18%) (Fig. 2F).

3.3. KEGG pathway analysis

To further verify the biological process of DEGs, we performed KEGG pathway analysis based on the whole-transcriptome background. P < 0.05 was set as cut-off value. As shown in Fig. 3A, various pathways, such as pathways of cancer, Huntington's disease, AD, MAPK signaling, and Neurotrophin signaling, were associated with identified DEGs. As a specific pathway, MAPK signaling pathway was closely related to AD. And various target genes of MAPK signaling pathway were involved in AD (Fig. 3B).

3.4. PPI network analyses and module analyses

Construction of a co-occurrence network was based on the STRING database. There are a total of 392 nodes and 766 edges with a combined score > 0.7 in the PPI network (Supplement 2 - Fig. 1). After topology analysis, a protein molecule was identified with the filtering of degree > average criteria, and the resulting PPI network contained a total of 100 nodes and 374 edges (Supplement 2 - Fig. 2). After filtering the PPI network with a criteria of degree \geq 14, 8 central node genes, including RPS29, CREBBP, ANAPC10, ANAPC4, MAGOHB, TCEB2, RPL10A, and SEC61A1, were identified as top hub genes. The significant modules of DEGs with the score > 8 were further selected by Molecular Complex Detection (MCODE), of which the highest score module included 12

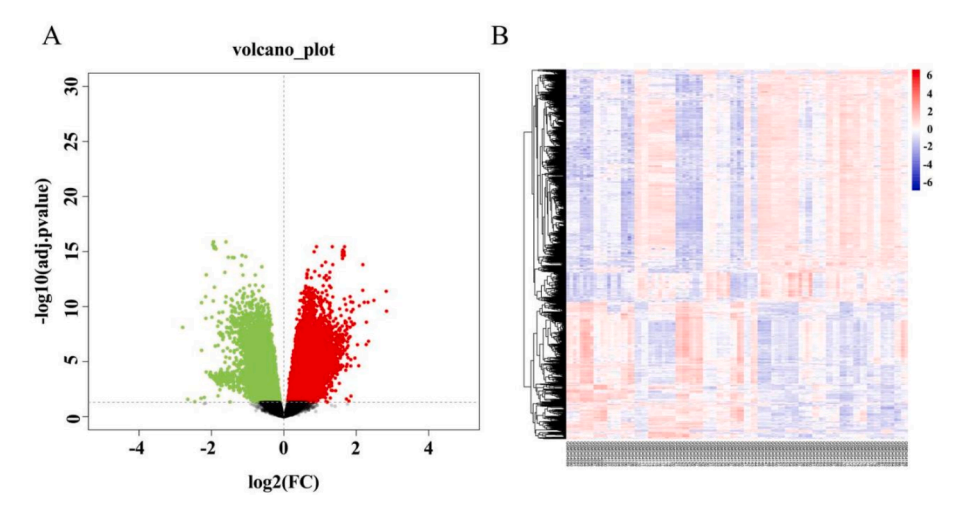


Fig. 1. The volcano plot and heatmap of DEGs in AD. A) The volcano plot of DEGs between AD and control samples. The red dots represent up-regulated genes, green dots represent down-regulated genes, and black dots represent genes not differentially expressed. B) The heatmap of top 100 up- and down-regulated genes (P < 0.05). Red ones represent upregulated genes and blue ones represent downregulated genes.

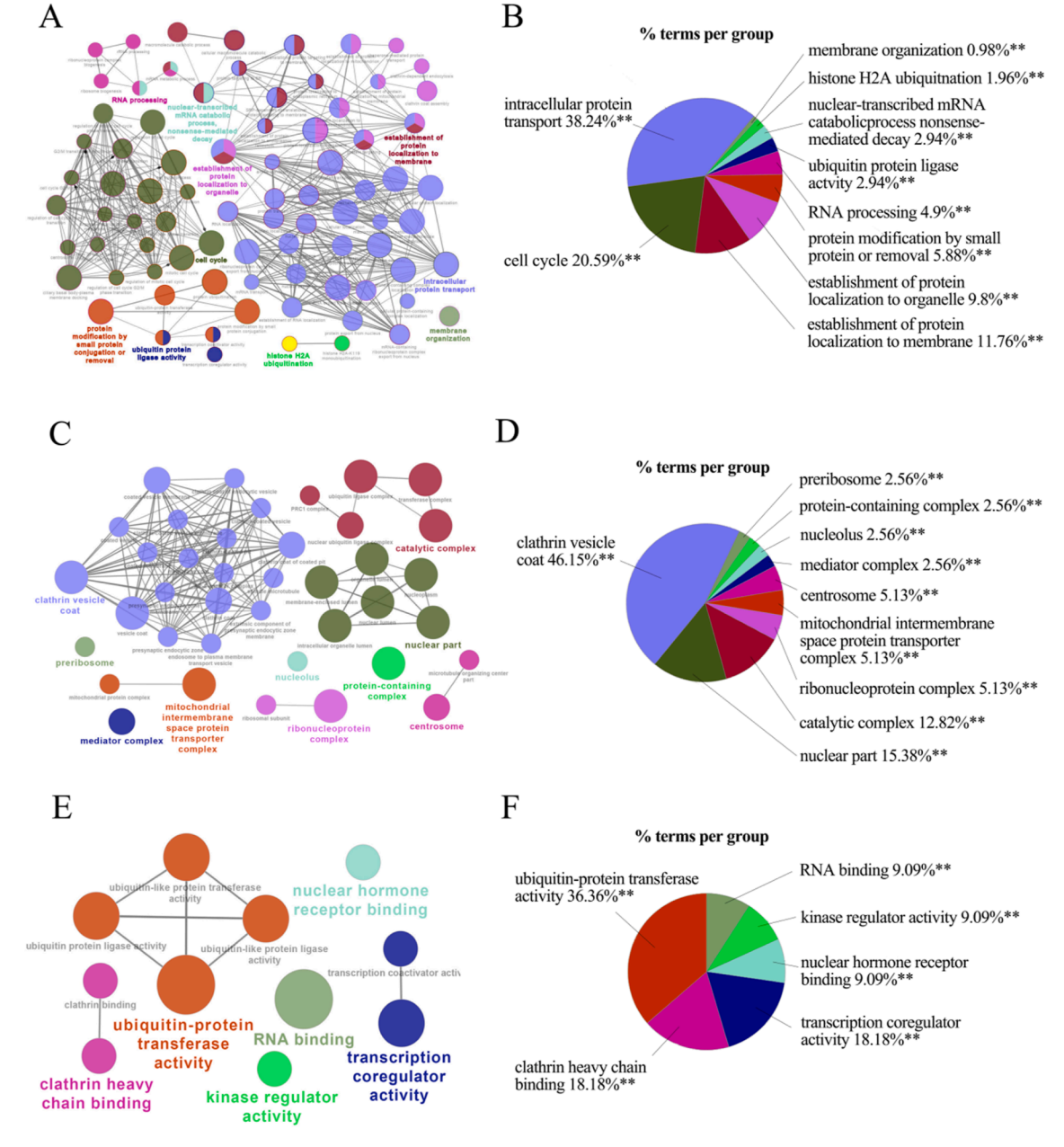


Fig. 2. GO enrichment analyses of identified DEGs in AD. A) Enrichment groups of GO Biological Process. B) Percentages of biological process terms per group. C) Enrichment groups of GO cellular components. D) Percentages of cellular component terms per group. E) Enrichment groups of GO molecular functions. F) Percentages of molecular function terms per group. **P < 0.01.

nodes and 66 edges (Fig. 4A). The second score module consisted of 18 nodes and 73 edges (Fig. 4B).

3.5. Drug-like small molecules analysis

The correlation coefficient score is an important parameter in the CMap database and ranges from -1 to 1. Positive values indicate a disease-promoting effect, whereas negative values indicate a disease-inhibiting effect. A larger absolute value represents a greater correlation between a small-molecule compound and disease. By topological differential gene mapping to the CMap database, negatively correlated small-molecule compounds with the highest correlation strength were screened out. Those with the top 12 scores are shown in Table 2; These compounds showed inhibitory effect on the expression of AD-related genes.

3.6. Morris water maze test

To test the spatial learning and memory deficits of animals, navigation tests and space probe tests were conducted. The findings showed that the escape latency greatly differed between the AD model group and sham model group, with the escape latency of the former significantly longer than that of the latter (P < 0.01) (Fig. 5A). A β_{1-42} -treated rats showed significantly fewer platform crossings compared to controls (Fig. 5A), confirming spatial memory deficit.

3.7. Expression of AD-related proteins

We also evaluated the expression of AD-related proteins of the hippocampus tissue in $A\beta_{1-42}$ -treated animals. Aberrant aggregated tau protein, phosphorylated tau in particular, is a hallmark of AD. ^{30,31} The

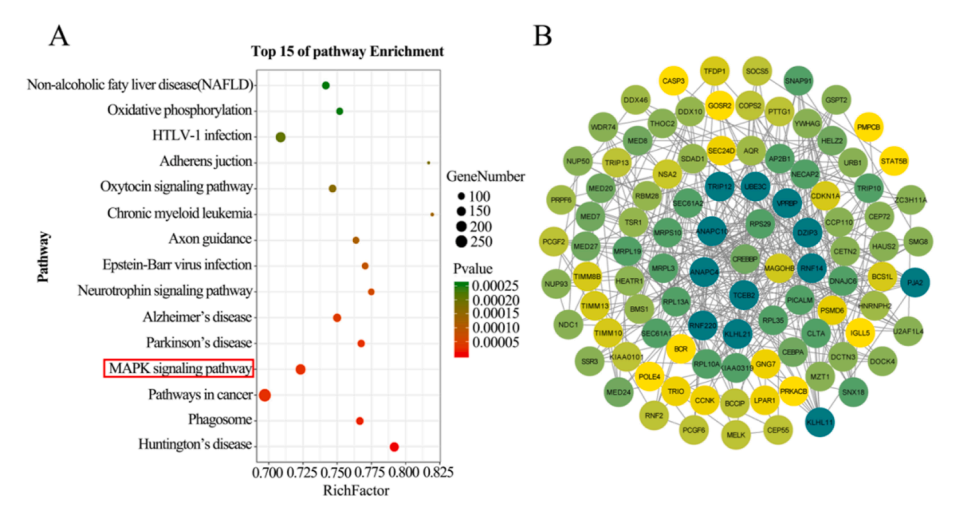


Fig. 3. KEGG pathway analysis of DEGs in AD. A) The top 15 enrichment KEGG pathways. The pathway maps were constructed by KEGG mapper. P < 0.001; B) Target genes of MAPK signaling pathway (hsa04010) involved in the AD.

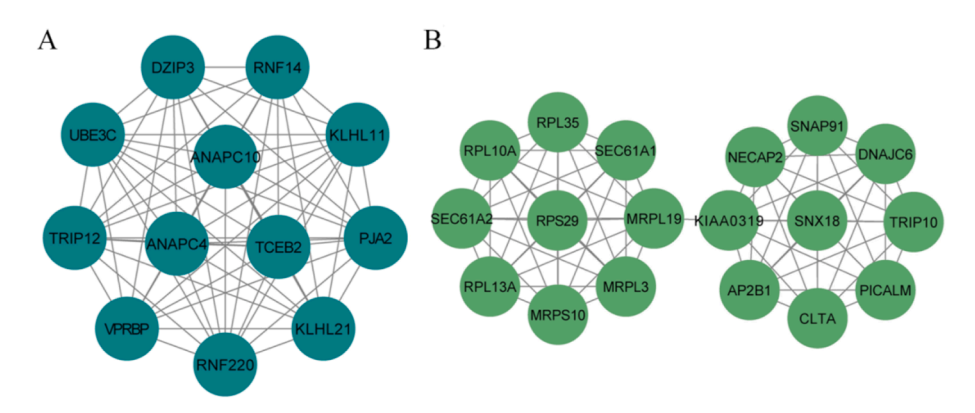


Fig. 4. Main clusters of protein-protein interaction networks of DEGs in AD. A) Module 1 from the PPI network (score > 12). B) Module 2 from the PPI network (score > 8).

amyloid plaques are the most striking lesions of AD, predominantly consisting of A β peptides, which were derived from the biological processing of proteolysis of the amyloid precursor protein (β APP). Consistent with AD pathology, A β_{1-42} -treated rats exhibited significant increases in phosphorylated tau and A β protein levels compared to controls (Fig. 5B). This result was also in agreement with the IHC analysis (Fig. 5C). Moreover, histological changes in hippocampus tissue were analyzed by H&E staining. As presented in Fig. 5C, A β_{1-42} -treated animals exhibited marked morphologic changes compared with the control.

Table 2Top 12 small molecule compounds with potential for treating AD.

CMap name	dose	cell	score	up	down
prochlorperazine	10 μΜ	MCF7	-1	-0.119	0.202
thioridazine	10 μΜ	MCF7	-0.967	-0.132	0.178
perhexiline	10 μΜ	MCF7	-0.952	-0.140	0.166
nortriptyline	13 μΜ	MCF7	-0.942	-0.132	0.171
fluoxetine	12 μΜ	MCF7	-0.939	-0.162	0.139
cinnarizine	11 μΜ	MCF7	-0.937	-0.139	0.161
clotrimazole	50 μM	MCF7	-0.926	-0.138	0.159
wortmannin	10 nM	MCF7	-0.922	-0.123	0.173
disopyramide	12 μM	MCF7	-0.919	-0.15	0.145
estradiol	10 nM	HL60	-0.916	-0.203	0.091
procarbazine	16 μΜ	HL60	-0.915	-0.22	0.073
15-delta prostaglandin J2	10 μΜ	MCF7	-0.909	-0.14	0.151

3.8. Validation of mRNA levels of hub genes

Next, a real-time PCR array was conducted to assess the mRNA levels of 8 crucial genes identified in the cerebral cortex. Compared to the control group, the mRNA level of CREBBP in AD rats was significantly increased (P < 0.01), whereas the mRNA level of the other seven genes showed no conspicuous alteration (Fig. 6). Therefore, we performed the following molecular docking between CREBBP and the small-molecule compounds.

3.9. Molecular docking

Semi-flexible docking was performed to optimize the docking parameters and define the flexible residues used in subsequent steps. The DS was applied to analyze ligand-protein interactions. Next, flexible residues in CREBBP with the 12 small-molecule compounds were designated (Supplement 2 - Fig. 3). Compared with semi-flexible docking, flexible docking more accurately calculates intermolecular interactions. According to BE of flexible docking, the top 6 of 12 molecules were prochlorperazine, cinnarizine, thioridazine, clotrimazole, nortriptyline, and wortmannin, showing binding energy of $-8.08,\,-6.41,\,-6.34,\,-5.36,\,-5.16,$ and -5.02, respectively, indicating that they strongly bind with CREBBP (Fig. 7). Among the 6 small-molecule compounds with greater binding ability, prochlorperazine showed the strongest binding and best treatment effect on AD according to CMap, indicating that prochlorperazine has the greatest potential to inhibit CREBBP.

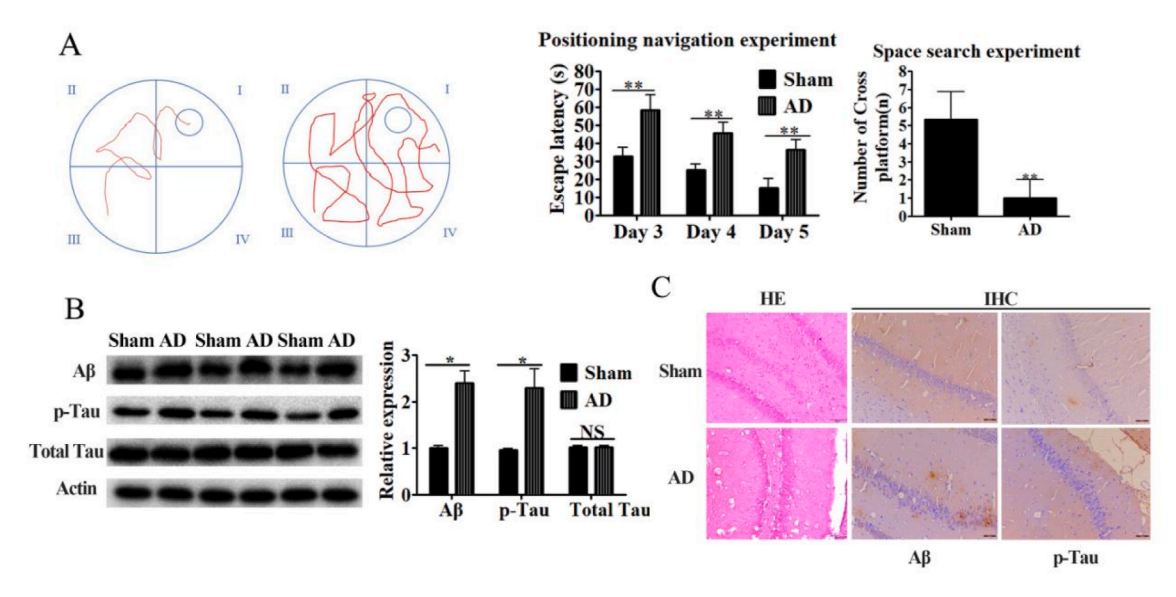


Fig. 5. Alteration of behavior, representative proteins, and histology in $A\beta_{1-42}$ -treated animals. A) Morris water maze test; Left panel: representative images of the swim paths; Right panel: escape latency in positioning navigation experiment and space search experiment. B.C) Proteins and histological change in hippocampus tissue, $A\beta$ and p-Tau expression level in $A\beta_{1-42}$ -treated and sham groups. *P < 0.05, **P < 0.01.

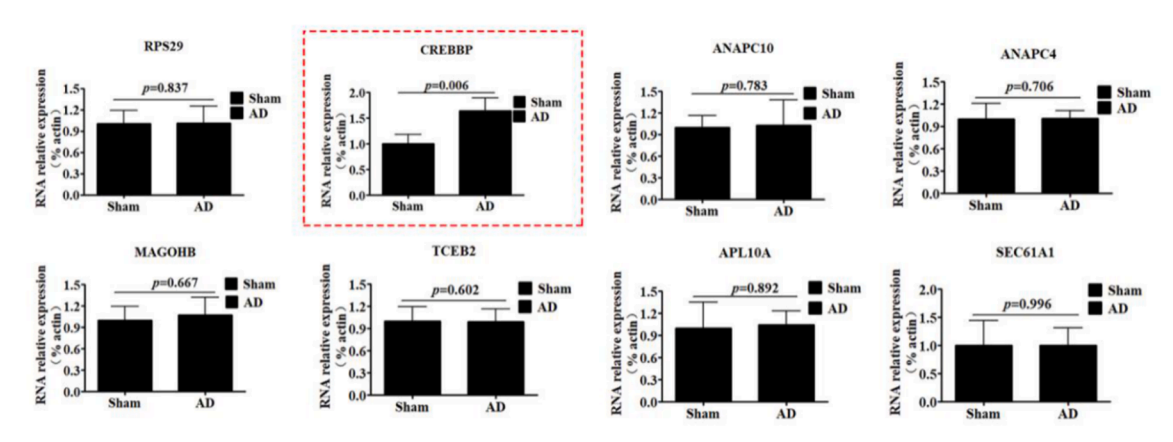


Fig. 6. Validation of the expression of crucial genes. Total RNA was isolated from the hippocampus tissue of $A\beta_{1-42}$ -treated rats and used for real-time PCR analysis to screen the expression of RPS29, CREBBP, ANAPC10, ANAPC4, MAGOHB, TCEB2, APL10A, and SEC1A1; n=5 per group. *P<0.05, **P<0.01.

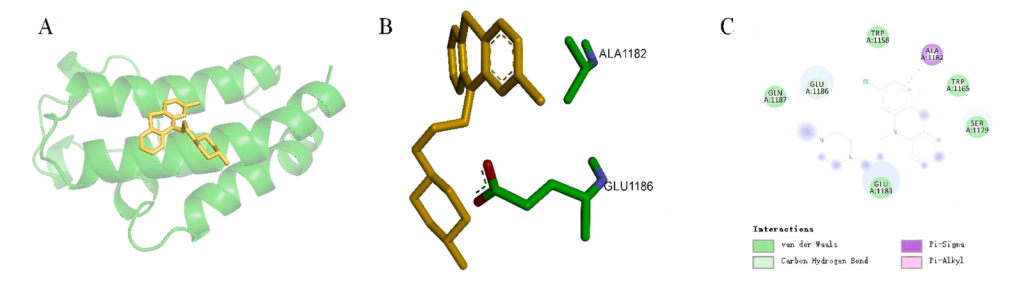


Fig. 7. The location and interaction between CREBBP and prochlorperazine. After flexible docking, the location and interaction between CREBBP and prochlorperazine were exhibited as cartoons (A), sticks (B), and two-dimensional interacting diagrams (C). CREBBP and drug molecules were colored in green and yellow, respectively.

4. Discussion

In the present study, we identified 1445 DEGs between AD patients and non-demented control samples, including 909 upregulated genes and 536 downregulated genes. Functional annotation through GO term analysis revealed that these DEGs are significantly enriched in biological processes related to intracellular protein transport and protein

localization to membranes, suggesting their involvement in AD pathogenic mechanisms. These findings align with previous studies indicating that protein trafficking and localization play crucial roles in AD pathophysiology.³³

Pathway enrichment analysis using KEGG further demonstrated that the identified DEGs are predominantly associated with nervous system disorders. Notably, the MAPK signaling pathway was significantly enriched in AD patients. Previous studies have shown that activation of MARK signaling is closely related to AD progression. ³⁴ MAPKs, a group of evolutionarily conserved serine/threonine protein kinases, are activated by extracellular stimuli and mediate signal transduction from the cell membrane to the nucleus. ³⁵ Activation of p38 MAPK induces tau hyperphosphorylation—a hallmark of AD neuropathology—while its inhibition improves cognitive function in animal models, ³⁵ underscoring its potential as a therapeutic target for cognitive dysfunction.

From PPI network analyses, we identified eight hub genes (RPS29, CREBBP, ANAPC10, ANAPC4, MAGOHB, TCEB2, RPL10A, and SEC61A1) based on their high connectivity degrees. Subsequent experimental validation in an AD rat model, however, revealed that only CREBBP exhibited consistent upregulation at the mRNA level, while the other seven candidates did not show significant changes. This discrepancy underscores the complementary nature of bioinformatic predictions and experimental validation, highlighting that computational approaches serve as powerful tools for identifying potential targets, whereas experimental confirmation remains essential for establishing biological relevance.

Using CMap platform, we screened several small-molecule compounds with potential anti-AD effects. Among these, prochlorperazine demonstrated the highest binding affinity for CREBBP in molecular docking studies (-8.08 kcal/mol). Although primarily known as a dopamine D2 receptor antagonist, ³⁶ prochlorperazine's strong interaction with CREBBP suggests its potential for repurposing in AD treatment. However, translational applications must consider its pharmacological profile, particularly the risk of extrapyramidal symptoms in elderly patients. 37-39 To address these limitations, we propose a multifaceted development strategy including dose optimization, structural modification to reduce D2 receptor affinity while preserving CREBBP binding, and exploration of adjunctive therapies targeting complementary pathways. While the study by Wen et al. also identified CREBBP as a potential AD target, 40 their research focused primarily on computational predictions without experimental validation in the context of environmental toxicology. In contrast, our study provides integrated bioinformatic and experimental evidence supporting CREBBP's role in AD pathogenesis and identifies prochlorperazine as a promising therapeutic candidate through comprehensive molecular docking analyses.

This study has certain limitations. First, the experimental validation was conducted only at the mRNA level, without assessment of protein expression. As gene expression is subject to post-transcriptional and translational regulation, changes at the mRNA level may not fully reflect protein abundance or activity. Consequently, the lack of protein-level confirmation may restrict the strength of our conclusions. In future work, additional experiments such as Western blotting, immunohistochemistry, or proteomics will be performed to validate the expression and biological function of the identified candidate genes at the protein level, thereby providing more comprehensive evidence.

In addition to these molecular-level limitations, the regional specificity of our transcriptional data also warrants careful consideration. While our study focused on cortical transcriptomic alterations in AD using the GSE122063 dataset, we recognize the importance of considering molecular changes across multiple brain regions in AD pathogenesis. Emerging evidence reveals both convergent and divergent molecular patterns between cortical and hippocampal regions that warrant discussion. At the systems level, certain molecular pathways (e. g., synaptic dysfunction, inflammatory responses) show consistent dysregulation across brain regions, 41 suggesting shared mechanisms of neurodegeneration. However, detailed transcriptomic analyses have identified striking regional specificity - cortical regions predominantly exhibit alterations in immune regulation and epigenetic modulation genes, while hippocampal regions show distinct changes in neurogenesis and glial differentiation pathways. 42 Our current cortical findings should therefore be interpreted as revealing one important component of AD's complex molecular landscape. The identified DEGs and hub genes (particularly CREBBP) may represent either: 1) pan-regional changes common to multiple affected areas, or 2) cortex-specific alterations contributing to the cognitive and behavioral manifestations of AD. Thus, while our mRNA-level analysis provides valuable insights, future studies incorporating multi-region sampling and single-cell transcriptomic approaches will be essential to elucidate the spatiotemporal dynamics of CREBBP expression and its role in neural circuit dysfunction in AD, complementing the protein-level validation suggested above.

5. Conclusion

In conclusion, our multi-level approach combining bioinformatics, experimental validation, and molecular docking supports CREBBP as a central regulator in AD and identifies prochlorperazine as a potential therapeutic agent. Further investigations are warranted to elucidate the precise mechanisms underlying CREBBP's involvement in AD pathogenesis and to optimize prochlorperazine for clinical applications.

CRediT authorship contribution statement

Jiaorong Zheng: Writing – original draft, Visualization, Validation, Methodology, Investigation, Formal analysis, Data curation. Deti Peng: Writing – original draft, Visualization, Validation, Methodology, Investigation, Formal analysis, Data curation. Zhigao Liao: Methodology, Resources, Validation, Writing – review & editing. Min Hong: Supervision, Resources, Project administration. Weiqu Yuan: Writing – review & editing, Supervision, Methodology, Funding acquisition, Conceptualization. Danping Huang: Writing – review & editing, Supervision, Methodology, Funding acquisition, Conceptualization.

Ethical approve

All animal experiment procedures using rats were approved by the Animal Experiment Administration Committee of Hubei University of Traditional Chinese Medicine (No. 42000600030515).

Funding

This work was supported by the Guangdong Basic and Applied Basic Research Foundation (No. 2022A1515110806), the National Natural Science Foundation of China (No. 82305181), and the Basic and Applied Basic Research Project of Guangzhou City (No. 2024A04J5054).

Declaration of interest statement

The authors declare that they have no known competing financial interests or personal relationships that could have appeared to influence the work reported in this paper.

Appendix A. Supplementary data

Supplementary data to this article can be found online at https://doi.org/10.1016/j.jhip.2025.09.005.

References

- 1. Arvanitakis Z, Bennett DA. What is dementia? JAMA. 2019 5;322(17):1728.
- Arvanitakis Z, Shah RC, Bennett DA. Diagnosis and management of dementia: review. *JAMA*. 2019;322(16):1589–1599.
- 3. Hou Y, Dan X, Babbar M, et al. Ageing as a risk factor for neurodegenerative disease. *Nat Rev Neurol.* 2019;15(10):565–581.
- Jessen F. Refining the understanding of typical alzheimer disease. Nat Rev Neurol. 2019;15(11):623-624.
- Wang K, Li M, Bucan M. Pathway-based approaches for analysis of genomewide association studies. Am J Hum Genet. 2007;81(6):1278–1283.
- 6. Ramanan VK, Kim S, Holohan K, et al. Alzheimer's disease neuroimaging initiative (ADNI). Genome-wide pathway analysis of memory impairment in the Alzheimer's disease neuroimaging initiative (ADNI) cohort implicates gene candidates, canonical pathways, and networks. Brain Imaging Behav. 2012;6(4):634–648.

- Zhang B, Gaiteri C, Bodea LG, et al. Integrated systems approach identifies genetic nodes and networks in late-onset alzheimer's disease. Cell. 2013;153(3):707–720.
- Schleinitz N, Chiche L, Guia S, et al. Pattern of DAP12 expression in leukocytes from both healthy and systemic lupus erythematosus patients. PLoS One. 2009;4(7): e6264.
- Atri A, Frölich L, Ballard C, et al. Effect of idalopirdine as adjunct to cholinesterase inhibitors on change in cognition in patients with alzheimer disease: three randomized clinical trials. *JAMA*. 2018;319(2):130–142.
- Rangaraju S, Dammer EB, Raza SA, et al. Identification and therapeutic modulation of a pro-inflammatory subset of disease-associated-microglia in alzheimer's disease. Mol Neurodegener. 2018;13(1):24.
- Yang B, Xia ZA, Zhong B, et al. Distinct hippocampal expression profiles of long noncoding RNAs in an alzheimer's disease model. *Mol Neurobiol*. 2017;54(7): 4833–4846.
- 12. Morris GM, Lim-Wilby M. Molecular docking. Methods Mol Biol. 2008;443:365-382.
- Hassan M, Shahzadi S, Seo SY, et al. Molecular docking and dynamic simulation of AZD3293 and solanezumab effects against BACE1 to treat Alzheimer'S disease. Front Comput Neurosci. 2018;12:34.
- Zhou A, Hu J, Wang L, et al. Combined 3D-QSAR, molecular docking, and molecular dynamics study of tacrine derivatives as potential acetylcholinesterase (AChE) inhibitors of alzheimer's disease. J Mol Model. 2015;21(10):277.
- McKay EC, Beck JS, Khoo SK, et al. Peri-infarct upregulation of the oxytocin receptor in vascular dementia. J Neuropathol Exp Neurol. 2019;78(5):436–452.
- Barrett T, Wilhite SE, Ledoux P, et al. NCBI GEO: archive for functional genomics data sets-update. Nucleic Acids Res. 2013;41(Database issue):D991-D995.
- Saddala MS, Lennikov A, Bouras A, et al. RNA-Seq reveals differential expression profiles and functional annotation of genes involved in retinal degeneration in Pde6c mutant Danio rerio. BMC Genom. 2020;21(1):132.
- Saddala MS, Lennikov A, Huang H. RNA-seq data from C-X-C chemokine receptor type 5 (CXCR5) gene knockout aged mice with retinal degeneration phenotype. *Data Brief.* 2020;31:105915.
- Shannon P, Markiel A, Ozier O, et al. Cytoscape: a software environment for integrated models of biomolecular interaction networks. *Genome Res.* 2003;13(11): 2498–2504
- Bindea G, Galon J, Mlecnik B. CluePedia Cytoscape plugin: pathway insights using integrated experimental and in silico data. *Bioinformatics*. 2013;29(5):661–663.
- Szklarczyk D, Gable AL, Lyon D, et al. STRING v11: protein-protein association networks with increased coverage, supporting functional discovery in genome-wide experimental datasets. *Nucleic Acids Res.* 2019;47(D1):D607–D613.
- Freilich R, Arhar T, Abrams JL, et al. Protein-protein interactions in the molecular chaperone network. Acc Chem Res. 2018;51(4):940–949.
- Hurle MR, Yang L, Xie Q, et al. Computational drug repositioning: from data to therapeutics. Clin Pharmacol Ther. 2013;93(4):335–341.
- Xia Z, Peng W, Cheng S, et al. Naoling decoction restores cognitive function by inhibiting the neuroinflammatory network in a rat model of alzheimer's disease. Oncotarget. 2017;8(26):42648–42663.
- Alkadhi KA, Dao AT. Exercise decreases BACE and APP levels in the hippocampus of a rat model of alzheimer's disease. Mol Cell Neurosci. 2018;86:25–29.

- Deng Y, Zhang J, Sun X, et al. miR-132 improves the cognitive function of rats with alzheimer's disease by inhibiting the MAPK1 signal pathway. Exp Ther Med. 2020;20 (6):159.
- Chu H, Zhang A, Han Y, et al. Metabolomics approach to explore the effects of kaixin-san on alzheimer's disease using UPLC/ESI-Q-TOF mass spectrometry. *J Chromatogr, B: Anal Technol Biomed Life Sci.* 2016;1015–1016:50–61.
- Morris GM, Huey R, Lindstrom W, et al. AutoDock4 and AutoDockTools4: automated docking with selective receptor flexibility. *J Comput Chem.* 2009;30(16): 2785–2791.
- Mitra S, Dash R. Structural dynamics and quantum mechanical aspects of shikonin derivatives as CREBBP bromodomain inhibitors. J Mol Graph Model. 2018;83:42–52.
- 30. Han P, Serrano G, Beach TG, et al. A quantitative analysis of brain soluble tau and the tau secretion factor. *J Neuropathol Exp Neurol*. 2017;76(1):44–51.
- Guthrie CR, Greenup L, Leverenz JB, et al. MSUT2 is a determinant of susceptibility to tau neurotoxicity. Hum Mol Genet. 2011;20(10):1989–1999.
- 32. Nunan J, Small DH. Regulation of APP cleavage by alpha-, beta- and gammasecretases. FEBS Lett. 2000;483(1):6–10.
- Sanders AE, Wang C, Katz M, et al. Association of a functional polymorphism in the cholesteryl ester transfer protein (CETP) gene with memory decline and incidence of dementia. JAMA. 2010:303(2):150–158.
- Park JS, Lee J, Jung ES, et al. Brain somatic mutations observed in alzheimer's disease associated with aging and dysregulation of tau phosphorylation. Nat Commun. 2019;10(1):3090.
- Kyriakis JM, Avruch J. Mammalian MAPK signal transduction pathways activated by stress and inflammation: a 10-year update. *Physiol Rev.* 2012;92(2):689–737.
- Tashiro M, Naito T, Kagawa Y, et al. Simultaneous determination of prochlorperazine and its metabolites in human plasma using isocratic liquid chromatography tandem mass spectrometry. *Biomed Chromatogr.* 2012;26(6): 754-760
- Sykes DA, Moore H, Stott L, et al. Extrapyramidal side effects of antipsychotics are linked to their association kinetics at dopamine D2 receptors. *Nat Commun.* 2017;8 (1):763.
- **38.** de Greef R, Maloney A, Olsson-Gisleskog P, et al. Dopamine D2 occupancy as a biomarker for antipsychotics: quantifying the relationship with efficacy and extrapyramidal symptoms. *AAPS J.* 2011;13(1):121–130.
- Iyo M, Tadokoro S, Kanahara N, et al. Optimal extent of dopamine D2 receptor occupancy by antipsychotics for treatment of dopamine supersensitivity psychosis and late-onset psychosis. J Clin Psychopharmacol. 2013;33(3):398–404.
- Wen J, Hu J, Yang X, et al. Effective analysis of alzheimer's disease and mechanisms of methyl-4-hydroxybenzoate using network toxicology, molecular docking, and machine learning strategies. Curr Alzheimer Res. 2025.
- Kim YJ, Cho H, Kim YJ, et al. Apolipoprotein e4 affects topographical changes in hippocampal and cortical atrophy in alzheimer's disease dementia: a five-year longitudinal study. J Alzheimers Dis. 2015;44(4):1075–1085.
- Tan PK, Ananyev E, Hsieh PJ. Distinct genetic signatures of cortical and subcortical regions associated with human memory. eNeuro. 2019;6(6). ENEURO.0283-19,2019.